Journal of Sound and Vibration (1999) **228**(3), 629–650
Article No. jsvi.1999.2422, available online at http://www.idealibrary.com on IDEAL®

LQG/GA DESIGN OF ACTIVE NOISE CONTROLLERS FOR A COLLOCATED ACOUSTIC DUCT SYSTEM

JONG-YIH LIN, HORNG-YIH SHEU AND SHIH-CHENG CHAO

Department of Mechanical Engineering, National Chung Hsing University, Taichung, Taiwan, R.O.C.

(*Received* 21 *October* 1997, *and in final form* 7 *June* 1999)

Active noise control of an acoustic duct system is studied by a real state-space model in this paper. The linear quadratic Gaussian (LQG) method is chosen to design an active noise controller in order to reject noise in a collocated duct system subject to a disturbance source at one end. Robustness property of the designed controller with respect to the uncertainty of a complex-valued acoustic impedance at the other end is validated through computer simulations. A nominal real-valued acoustic impedance is therefore used to design reduced order controllers. The design parameters of the LQG method are automatically adjusted by using a simple genetic algorithm (SGA) to achieve a better global control effect. This adjustment is guided by a fitness function of SGA specified by a control objective. Results from computer simulation demonstrate the global effectiveness of the active noise controllers. Results of experiments also support the feasibility of the proposed design method.

1. INTRODUCTION

Acoustic noise has become an important issue in our society, primarily due to the health concerns of exposure to acoustic noise. A low level of acoustic noise is often a requisite for places such as factories, offices and mufflers contain duct assemblies. Passive techniques such as the use of absorbent materials can generally reduce high-frequency noise but not low-frequency noise. Instead, active noise controllers are required to lessen low-frequency noise.

Several strategies for active noise control have been established. One is to utilize various adaptive filters [1–5] to cancel noise at one or more specific measurement locations monitored by microphones but other areas that are not measured usually result in increasing noise. Cancellation of acoustic noise has been only limited to one point or small region of the duct. Others use modern feedback control theorems to design feedback controllers that can provide global noise reduction of acoustic duct systems; a transfer function model of a finite-length duct [6] and a complex state-space model [7] have recently been developed. Nevertheless, the outputs of these two models are generally of complex values and are not directly detectable. Only their real parts can be detected with physical sensors such as microphones. This may generate inconsistency between feedback control design and implementation.

0022-460X/99/480629 + 22 $30.00/0

In this paper, a real state-space model of a one-dimensional acoustic duct is obtained by modifying the result in reference [8], and is used for the study of active noise control. The linear quadratic Gaussian (LQG) method [9, 10] is chosen to design feedback controllers to achieve global noise reduction. The design parameters of the LQG method are automatically tuned by using a simple genetic algorithm (SGA) since genetic algorithms have been established as a useful technique in search and optimization [11, 12] and in control [13, 14]. The LQG design method combined with a simple genetic algorithm is therefore referred to as LQG/GA.

2. SYSTEM MODEL

A hard-walled, one-dimensional duct system is modelled as [15, 16]

$$\frac{\partial^2 w(z,t)}{\partial t^2} - c^2 \frac{\partial^2 w(z,t)}{\partial z^2} = -\frac{\partial}{\partial z}\left[\frac{\delta(z)P(t)}{\rho}\right] - \delta(z - z_i)\frac{\partial}{\partial t}\left[\frac{M(t)}{\rho S}\right], \tag{1}$$

where $w(z, t)$ is the particle displacement (m), t the time (s), c the wave speed (340 m/s), ρ the density of the medium (1·225 kg/m^3), $\delta(x)$ the Dirac delta function, $P(t)$ the pressure excitation at $z = 0$ (N/m^2), $M(t)$ the mass flow input in the domain at z_i (kg/s), S the area of the mass flow input (m^2), and z_i the input location (m).

The associated boundary conditions are

$$\frac{\partial w(0,t)}{\partial z} = 0, \tag{2}$$

$$\frac{\partial w(L,t)}{\partial z} = -\frac{K}{c}\frac{\partial w(L,t)}{\partial t}, \quad K \neq 0 + 0i,\ 1 + 0i,\ \infty, \tag{3}$$

where L is the length of the duct (m), K the complex impedance of the termination end (dimensionless) and $i = \sqrt{-1}$.

The acoustic pressure of the duct system is obtained as

$$P(z_m, t) = -\rho c^2 \frac{\partial w(z,t)}{\partial z}\bigg|_{z = z_m}, \tag{4}$$

where z_m is the measured location (m).

Define

$$\frac{1}{2L}\ln\left(\frac{1-K}{1+K}\right) = \alpha + i\gamma, \tag{5}$$

$$\beta_n = -\frac{n\pi}{L}, \quad n = 0,\ \pm 1,\ \pm 2, \ldots, \tag{6}$$

where α, γ and β_n are of real values. Consider that the pressure excitation $P(t)$ and the mass flow input $\partial M(t)/\partial t$ are produced by physical devices such as speakers and thus they are assumed to be of real values. Further consider sensors such are microphones that can only detect the real part of the acoustic pressure $P(z_m, t)$. Therefore define disturbance noise d, control input u and measured output y_r as

$$d(t) = P(t), \quad u(t) = \frac{\partial M(t)}{\partial t}, \quad y(t) = P(z_m, t), \quad y_r(t) = \mathrm{Re}[y(t)].$$

A real state-space model of an acoustic duct system is developed in Appendix A and is then described as

$$\dot{x}_n = A_n x_n + B_n u + G_n d, \quad n = 0, 1, 2, \ldots, \tag{7}$$

$$y_r = \sum_{n=0}^{\infty} C_n x_n, \tag{8}$$

where

$$x_n = \begin{bmatrix} \bar{x}_{nr} \\ \bar{x}_{ni} \end{bmatrix}, \quad A_n = \begin{bmatrix} \bar{A}_{nr} & -\bar{A}_{ni} \\ \bar{A}_{ni} & \bar{A}_{nr} \end{bmatrix}, \quad B_n = \begin{bmatrix} \bar{B}_{nr} \\ \bar{B}_{ni} \end{bmatrix}, \quad G_n = \begin{bmatrix} \bar{G}_n \\ 0 \end{bmatrix}, \quad C_n^{\mathrm{T}} = \begin{bmatrix} \bar{C}_{nr}^{\mathrm{T}} \\ -\bar{C}_{ni}^{\mathrm{T}} \end{bmatrix}.$$

For control design and computer simulation, a finite-order matrix formulation is obtained with $n = 0, 1, 2, \ldots, N$ in equations (7)–(8) as

$$\dot{x} = Ax + Bu + Gd, \qquad y_r = Cx, \tag{9, 10}$$

where

$$x = \begin{bmatrix} x_0 \\ x_1 \\ \vdots \\ x_N \end{bmatrix}, \quad A = \begin{bmatrix} A_0 & & & \\ & A_1 & \underline{0} & \\ & \underline{0} & \ddots & \\ & & & A_N \end{bmatrix},$$

$$B = \begin{bmatrix} B_0 \\ B_1 \\ \vdots \\ B_N \end{bmatrix}, \quad G = \begin{bmatrix} G_0 \\ G_1 \\ \vdots \\ G_N \end{bmatrix}, \quad C^{\mathrm{T}} = \begin{bmatrix} C_0^{\mathrm{T}} \\ C_1^{\mathrm{T}} \\ \vdots \\ C_N^{\mathrm{T}} \end{bmatrix}.$$

This system has an order of $(4N + 2)$. When $0 < K < 1$, one has $\gamma = 0$ and $\alpha < 0$ from equation (5). This leads to $\bar{A}_{ni} = 0$, $\bar{B}_{ni} = 0$, $\bar{C}_{ni} = 0$ and stable $\bar{A}_{nr}$ for $n = 0, 1, 2, \ldots$. Hence, $\bar{x}_{ni}$ is uncontrollable from u, unobservable from y_r, and uncoupled to $\bar{x}_{nr}$. Further since $\bar{A}_{nr}$ is stable, $\bar{x}_{ni}$ can be neglected. After neglecting

all $\bar{x}_{ni}$ in equations (9)–(10), a simplified system of order of $(2N + 1)$ can be obtained as

$$\dot{x} = Ax + Bu + Gd, \qquad y_r = Cx, \tag{11, 12}$$

where

$$x = \begin{bmatrix} \bar{x}_{0r} \\ \bar{x}_{1r} \\ \vdots \\ \bar{x}_{Nr} \end{bmatrix}, \quad A = \begin{bmatrix} \bar{A}_{0r} & & & \\ & \bar{A}_{1r} & \underline{0} & \\ & \underline{0} & \ddots & \\ & & & \bar{A}_{Nr} \end{bmatrix},$$

$$B = \begin{bmatrix} \bar{B}_{0r} \\ \bar{B}_{1r} \\ \vdots \\ \bar{B}_{Nr} \end{bmatrix}, \quad G = \begin{bmatrix} \bar{G}_0 \\ \bar{G}_1 \\ \vdots \\ \bar{G}_N \end{bmatrix}, \quad C^{\mathrm{T}} = \begin{bmatrix} \bar{C}_{0r}^{\mathrm{T}} \\ \bar{C}_{1r}^{\mathrm{T}} \\ \vdots \\ \bar{C}_{Nr}^{\mathrm{T}} \end{bmatrix}.$$

3. LQG DESIGN OF ACTIVE NOISE CONTROLLERS

Active noise controllers for an acoustic duct system are designed based on the real state-space model of equations (9)–(10) where $N = N_d$. Generally, N_d is chosen to have a small value such that only modes of low frequencies of concern are included in the model. A nominal plant for the LQG design is formed by using this model with given process noise w and measurement noise v as

$$\dot{x} = Ax + Bu + w, \qquad y_r = Cx + v. \tag{13, 14}$$

Assume that w and v are Gaussian white noise processes with zero means and with covariance as

$$E\{ww^{\mathrm{T}}\} = Q_e \geqslant 0, \qquad E\{vv^{\mathrm{T}}] = R_e > 0, \qquad E\{wv^{\mathrm{T}}\} = 0.$$

Define a performance index as

$$J = \lim_{t \to \infty} \frac{1}{t} E\left\{ \int_0^t (x^{\mathrm{T}} Q_c x + u^{\mathrm{T}} R_c u)\, \mathrm{d}\tau \right\}. \tag{15}$$

Then the LQG controller can be obtained as

$$\dot{x}_c = (A - BK_c - K_f C)x_c + K_f y_r, \qquad u = -K_c x_c, \tag{16, 17}$$

where

$$K_c = R_c^{-1} B^{\mathrm{T}} P_c, \qquad K_f = P_e C^{\mathrm{T}} R_e^{-1},$$

where P_c and P_e satisfy the following Riccati equations:

$$0 = P_c A + A^{\mathrm{T}} P_c - P_c B R_c^{-1} B^{\mathrm{T}} P_c + Q_c,$$

$$0 = A P_e + P_e A^{\mathrm{T}} - P_e C^{\mathrm{T}} R_e^{-1} C P_e + Q_e,$$

respectively. Control objective is to have good disturbance rejection with respect to disturbance noise d by using the control input u in equations (11)–(12). Therefore, a given d_1 in the range of G is included in w. Given that truncated dynamics exits between a low order model design model and a high order applied model of a controller, u would be associated with a feature of some degree of uncertainty. A disturbance d_2 is thus given in the range of B and is included in w. Thus, let

$$w = G d_1 + B d_2,$$

where

$$E\{d_1 d_1^{\mathrm{T}}\} = q_{e1} \mathrm{I} \geqslant 0,$$

$$E\{d_2 d_2^{\mathrm{T}}\} = q_{e2} \mathrm{I} \geqslant 0.$$

It is reasonable to assume that d_2 and d_1 are uncorrelated since the associated u and d are generated by two different speakers in a real physical system. Then, the weights of the LQG design can be chosen as

$$Q_c = q C^{\mathrm{T}} C, \qquad R_c = 1, \tag{18, 19}$$

$$Q_e = q_{e1} G G^{\mathrm{T}} + q_{e2} B B^{\mathrm{T}}, \qquad R_e = 1. \tag{20, 21}$$

This reduces the LQG design parameters to q, q_{e1}, and q_{e2}.

For computer simulation, the designed LQG controller of equations (16)–(17) is applied to the acoustic duct system of equations (9)–(10) where $N = N_s$ and the system matrices are given as A_p, B_p, C_p, and G_p. In general, N_s is much larger than N_d. Define

$$x_s = \begin{bmatrix} x \\ x_c \end{bmatrix}.$$

The closed-loop system is then obtained as

$$\dot{x}_s = A_{ps} x_s + G_{ps} d, \qquad y_r = C_{ps} x_s, \tag{22, 23}$$

where

$$A_{ps} = \begin{bmatrix} A_p & -B_p K_c \\ K_f C_p & A - BK_c - K_f C \end{bmatrix}, \qquad G_{ps} = \begin{bmatrix} G_p \\ \underline{0} \end{bmatrix}, \qquad C_{ps} = [C_p \quad \underline{0}].$$

The designed controller is required not only to stabilize the acoustic duct system but also to achieve expected performance. Stability can be acquired if all the eigenvalues of A_{ps} have negative real parts. Computer simulation results indicate that this LQG method is useful to obtain stabilizing controller for a collocated structure, but not for a non-collocated structure due to truncated dynamics of a duct (data not shown). Thus, in the following, only the collocated case is considered. As for the performance, it can be evaluated in the frequency domain by using the closed-loop and the open-loop transfer functions as

$$T_{cl}(s) = \frac{\hat{y}_r^c(s)}{\hat{d}(s)} = C_{ps}(s\mathrm{I} - A_{ps})^{-1} G_{ps}, \tag{24}$$

$$T_{op}(s) = \left.\frac{\hat{y}_r^{uc}(s)}{\hat{d}(s)}\right|_{u=0} = C_p(s\mathrm{I} - A_p)^{-1} G_p, \tag{25}$$

where y_r^c and y_r^{uc} depict the y_r resulting from the closed-loop system and the open-loop system respectively, subject to the same disturbance noise d. Define transmission losses [17] as

$$L_{cl} \equiv 20 \log \frac{p_{cl}}{p_0} = 20 \log T_{cl}(i\omega) \quad \mathrm{dB},$$

$$L_{op} \equiv 20 \log \frac{p_{op}}{p_0} = 20 \log T_{op}(i\omega) \quad \mathrm{dB},$$

where p_0 is the amplitude of d and p_{cl} and p_{op} are the amplitudes of y_r for the closed-loop and the open-loop systems respectively. Further define insertion loss [17] as

$$L_{IL} \equiv 20 \log \frac{p_{cl}}{p_0} - 20 \log \frac{p_{op}}{p_0} = L_{cl} - L_{op} = 20 \log \frac{T_{cl}(i\omega)}{T_{op}(i\omega)} \quad \mathrm{dB}. \tag{26}$$

This insertion loss represents the level of noise attenuation in the duct for a sinusoidal disturbance of frequency ω at the measured location.

Now, consider that an acoustic duct system is of length $L = 1{\cdot}2$ m and has an acoustic impedance of $K = 0{\cdot}051 - 0{\cdot}0015i$. A control input and a measured

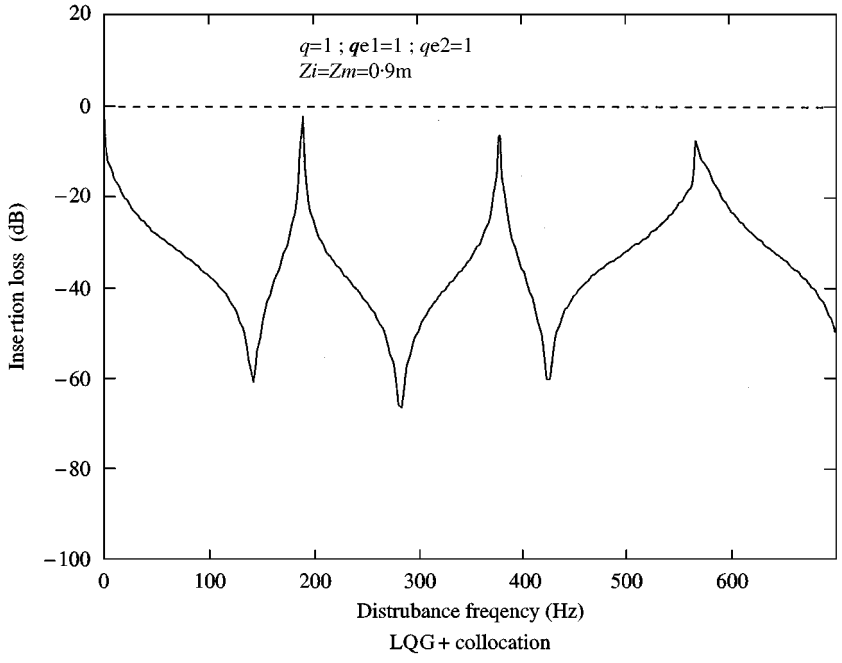

Figure 1. Insertion losses of a full order controller.

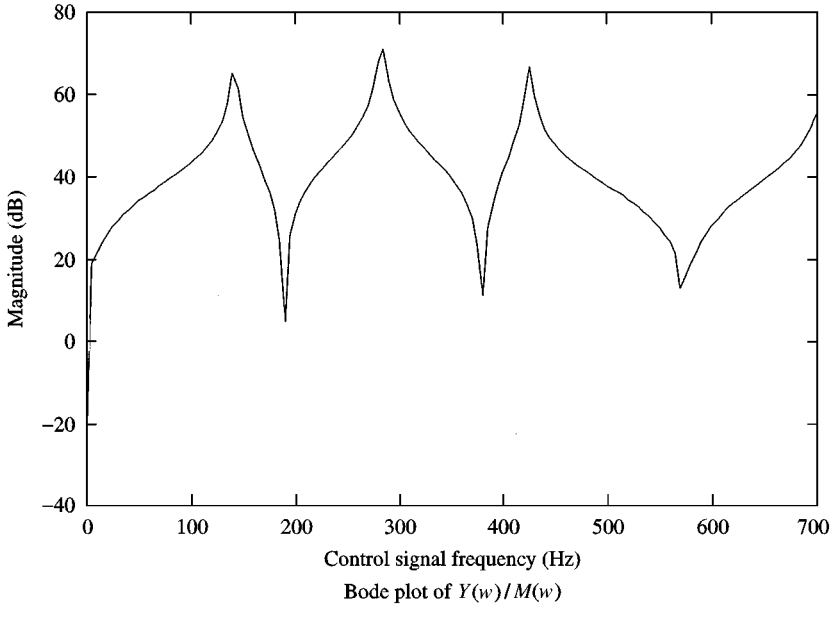

Figure 2. Bode plot of measured output to control input.

feedback output are collocated at $z_i = z_m = 0{\cdot}9$ m. The area of the control mass flow input is assumed to be $S = \pi 0{\cdot}075^2/4$ m^2. Let $N = N_d = 3$ in equations (9)–(10) for the LQG design and choose the design parameters as equations (18)–(21) where $q = 1$, $q_{e1} = 1$, $q_{e2} = 1$. This leads to an LQG controller of order 14. The designed

TABLE 1

Insertion losses (dB) of perturbing real part only

$K = 0{\cdot}04895$, $z_i = z_{ni} = 0{\cdot}9$ m		
K_p	150 Hz	190 Hz
0·001	− 54·56	− 5·91
0·01	− 54·56	− 5·87
0·05	− 54·29	− 5·72
0·10	− 53·51	− 5·54
0·20	− 51·37	− 5·20
0·30	− 49·32	− 4·92
0·40	− 47·64	− 4·71
0·50	Unstable	Unstable

controller is then used for computer simulation where the plant of order 162 is described by equations (9)–(10) and $N = N_s = 40$. For d of frequencies under 700 Hz, the insertion losses are lower than -20 dB for most of frequencies as shown in Figure 1 except for those frequencies near 0, 190, 380 and 570 Hz. This is because the control gains from u to y_r are much smaller at those frequencies as shown in Figure 2.

4. DESIGN OF ROBUST REDUCED ORDER CONTROLLERS

The acoustic impedance considered above is when $K = 0{\cdot}051 - 0{\cdot}0015i$, of which the imaginary part is small. Neglecting the imaginary part of the acoustic impedance in the LQG design may lead to the reduction of the controller order to half. However, one must consider the robustness characteristics with respect to the acoustic impedance.

Redesign of the active noise controller in the previous section using a nominal value as $K = 0{\cdot}051$ results in $\gamma = 0$ from equation (5). Thus, the simplified model of equations (11)–(12) and $N = N_d = 3$ is used for control design. A seventh order LQG controller is then obtained.

The 162th plant used for computer simulation in the previous section is used again here to test the performance of the seventh order controller. Control effects for disturbance noise of frequencies under 700 Hz are nearly identical to the results shown in Figure 1, indicating a very comparable performance between these two designs. This suggests that the neglect of the imaginary part of the acoustic impedance in the LQG control design is feasible and the reduced order controller is robust. To further test the robustness property, values of the acoustic impedance are perturbed in three different ways including perturbing K in its real part only (Table 1), perturbing K in its imaginary part only (Table 2), and perturbing K in both real and imaginary parts (Table 3). Insertion losses for all conditions are found to be $-37{\cdot}7$ dB or less for disturbance noise of 150 Hz and are $-4{\cdot}71$ dB or less for disturbance noise of 190 Hz. These results thus confirm that the reduced order

TABLE 2

Insertion losses (dB) of perturbing imaginary part only

$K = 0{\cdot}04895$, $z_i = z_{ni} = 0{\cdot}9$ m		
$\mathrm{Im}(K_p)$	150 Hz	190 Hz
$\pm$ 0·01	− 54·29	− 5·73
$\pm$ 0·1	− 56·03	− 5·73
$\pm$ 1·0	− 37·70	− 5·66
+ 10	− 39·29	− 6·74
$\pm$ 10 e3	− 39·31	− 6·73
$\pm$ 10 e5	− 39·31	− 6·73
$\pm$ 10 e7	Unstable	Unstable

TABLE 3

Insertion losses (dB) of perturbing both real and imaginary parts

$K = 0{\cdot}04895$, $z_i = z_{ni} = 0{\cdot}9$ m		
K_p	150 Hz	190 Hz
0·15 $\pm$ 0·1i	− 52·43	− 5·38
0·25 $\pm$ 0·2i	− 48·50	− 5·11
0·35 $\pm$ 0·3i	− 45·38	− 4·95
0·45 $\pm$ 0·4i	− 43·45	− 4·89
0·55 $\pm$ 0·5i	− 42·25	− 5·09
0·65 $\pm$ 0·6i	− 41·48	− 5·08
0·75 $\pm$ 0·7i	− 40·97	− 5·28
0·85 $\pm$ 0·8i	− 40·62	− 5·52
0·95 $\pm$ 0·9i	− 40·37	− 5·76

LQG design is robust with respect to the acoustic impedance and the truncated dynamics.

5. LQG/GA DESIGN

To obtain a better reduced LQG controller, the design parameters q, q_{e1} and q_{e2} have to be properly tuned. A simple genetic algorithm (SGA) [12] is adopted here and combined with the LQG design so as to be able to adjust the design parameters automatically (Figure 3). A SGA is specified by a fixed population and consists of reproduction, crossover, and mutation operators. A SGA works on a set of strings referred to as population. This population evolves from generation to generation through the application of genetic operators with probabilistic transition rules. Given intervals of design parameters are first encoded to unsigned integers of binary format with a certain of bits, say 15 bits. These binary integers are then

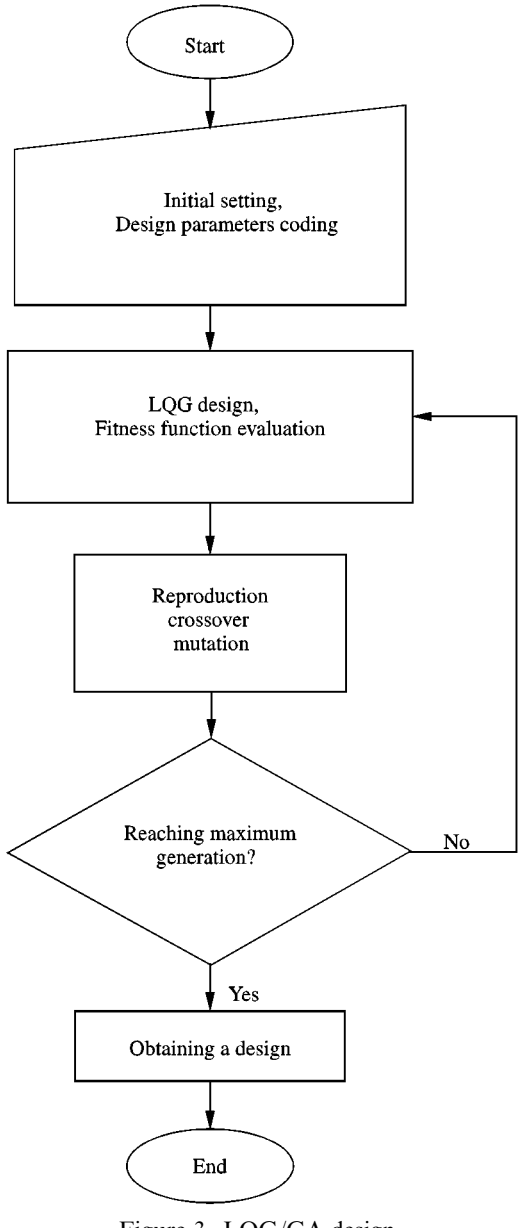

Figure 3. LQG/GA design.

cascaded to form a string that SGA can work on. The fitness function of the LQG/GA is defined by a control objective which is used to calculate a fitness, f_i, for each individual in the population. The weighted fitness, defined as $W_i = f_i/\sum f_i$ ($\sum_i W_i = 1$), forms a roulette wheel as shown Figure 4 which is used to determine the number of reproduction for each individual. This is based on the principle of survival of the fittest. After reproduction, all individuals in the population are mated randomly to each other as shown in Figure 5. The crossover site is also randomly selected. To avoid a search confined to a local region, mutation is then

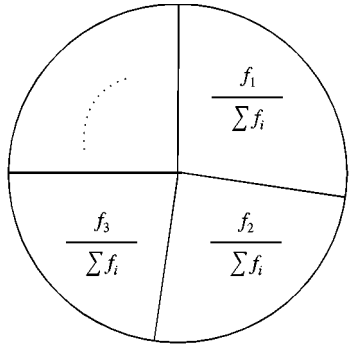

Figure 4. Roulett wheel.

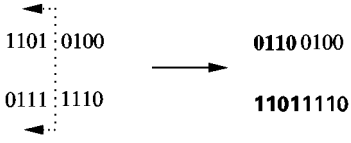

Figure 5. Crossover.

performed as shown in Figure 6 on a bit-by-bit basis and is applied with a low probability, say 1%. In binary strings, the mutation operator simply flips the state of a bit from 0 to 1 *vice versa*. After the genetic operations, a string is decomposed to binary integers of the corresponding design parameters. These binary integers are then decoded to the true values of the design parameters. At the end of the LQG/GA search, the best design parameters can be obtained.

Here reconsider the previous reduced order LQG controller design with a SGA to automatically search for the best design parameters according to the following fitness functions:

(1) Define a fitness function as

$$f = \begin{cases} M + \sum_{\omega_1}^{\omega_2} \left\{ \dfrac{|\hat{y}_r^{uc}(i\omega)| - |\hat{y}_r^{c}(i\omega)|}{|\hat{y}_r^{uc}(i\omega)|} \right\} & \text{if } A_{ps} \text{ stable,} \\ 0 & \text{if } A_{ps} \text{ unstable,} \end{cases} \tag{27}$$

where M is a positive number and is chosen to guarantee that f will always have a positive value, and ω_1 and ω_2 are the lower and upper bounds of frequencies of concern. Let $\omega_1 = 40$ Hz and $\omega_2 = 500$ Hz. In addition, let design parameters be restricted to

$$10^{-3} \leqslant q \leqslant 10^3, \qquad 10^{-3} \leqslant q_{e1} \leqslant 10^3, \qquad 10^{-3} \leqslant q_{e2} \leqslant 10^3.$$

Each design parameter is encoded by 15 bits of binary strings and then connected to form a string that a SGA can work on. Population is fixed as 30. Maximum

11010100

11000100

Figure 6. Mutation.

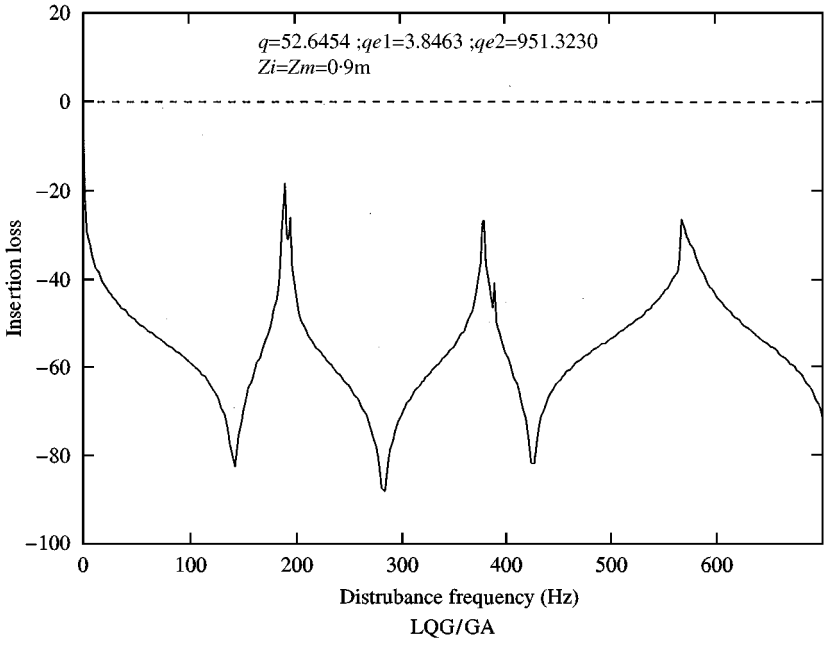

Figure 7. Insertion losses of a reduced order controller.

generation is 50. Operating through the SGA, a set of design parameters is obtained as

$$q = 52{\cdot}6454, \qquad q_{e1} = 3{\cdot}8463, \qquad q_{e2} = 951{\cdot}3230.$$

In this case, q_{e2} is obviously much larger than q_{e1}, reflecting that d_2 would be much greater than d_1 in this system, that is, most of the system noise would be from d_2 instead of d_1. As d_2 is considered as the disturbance from truncated dynamics, the significantly higher impact of d_2 seen here is possibly because a high level of truncated dynamics exists between the design model ($N = N_d = 3$) and the applied model ($N = N_s = 40$). As shown in Figure 7, better insertion losses of this controller for disturbance noise of frequencies under 700 Hz are obtained compared with those of the previous design.

(2) To globally reject a disturbance noise of frequency ω_c, define a fitness function as

$$f = \begin{cases} M + \sum_{o_1}^{o_n} \left\{ \dfrac{|\hat{y}_r^{uc}(i\omega_c, o_k)| - |\hat{y}_r^{c}(i\omega_c, o_k)|}{|\hat{y}_r^{uc}(i\omega_c, o_k)|} \right\} & \text{if } A_{ps} \text{ stable,} \\ 0 & \text{if } A_{ps} \text{ unstable,} \end{cases} \tag{28}$$

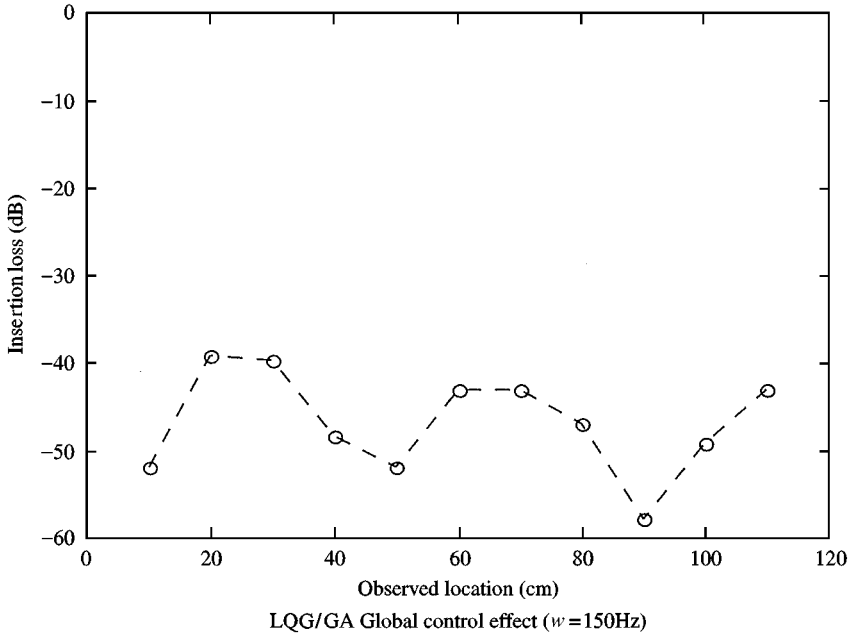

Figure 8. Global noise attenuation of a reduced order controller.

where $o_1 \sim o_n$ are locations of concern. Consider, $\omega_c = 150$ Hz and 11 positions located from 0·10 to 1·10 m along the 1·20-m duct at a 0·10-m interval are set up for monitoring. The collocated position of sensor and actuator is now considered as a design parameter in addition to the LQG design parameters. Confine these design parameters to be

$$10^{-3} \leqslant q \leqslant 10^3, \quad 10^{-3} \leqslant q_{e1} \leqslant 10^3, \quad 10^{-3} \leqslant q_{e2} \leqslant 10^3, \quad 0{\cdot}10 \leqslant z_i = z_m \leqslant 1{\cdot}10.$$

Again, each design parameter is encoded by 15 bits of binary strings. Population is 30 and maximum generation is 50. The best design parameters are obtained as

$$q = 285{\cdot}6540, \qquad q_{e1} = 147{\cdot}7715, \qquad q_{e2} = 492{\cdot}2335, \qquad z_i = z_m = 0{\cdot}10.$$

The collocated position of the control input and feedback sensor is found to be at 0·10 m which is the allowable nearest location to the disturbance. Insertion losses are lower than ~ -40 dB in all 11 locations as shown in Figure 8.

6. EXPERIMENT AND DISCUSSION

Experimental facility of an active control acoustic duct system was built using a 1·2-m long PVC circular tube (9·4-cm inner diameter and 10-cm outer diameter) as shown in Figure 9. A GW GFG-813 function generator was used to produce sinusoidal signals amplified by a King Sound Model-300B amplifier in order to derive a home-made speaker (8-cm diameter) at one end of the acoustic duct.

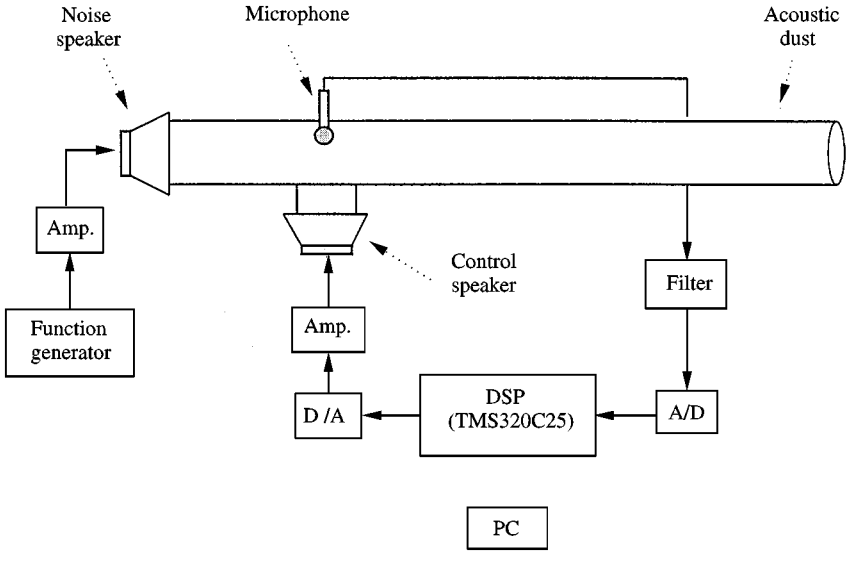

Figure 9. Experimental set-up for active noise control.

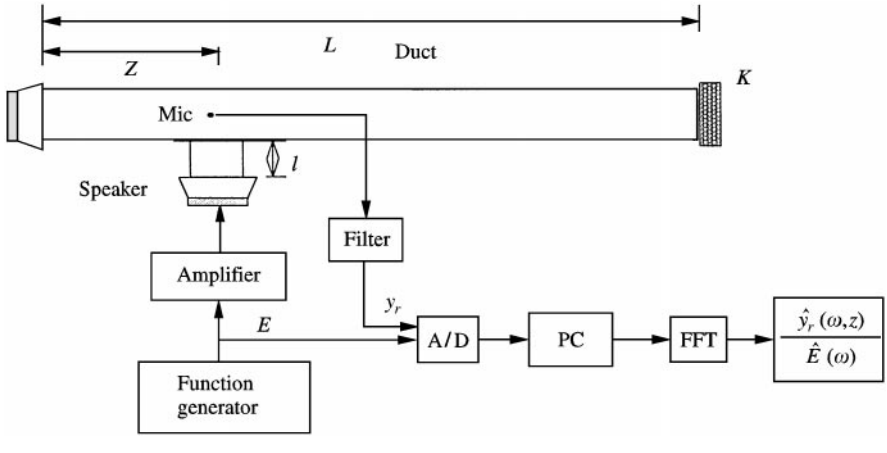

Figure 10. Frequency response evaluation of an actuating system.

Consequently, a sinusoidal disturbance noise source for the acoustic duct was generated. The other end of the duct was open to the air and it was characterized by an acoustic impedance experimentally identified to be $K = 0{\cdot}051 - 0{\cdot}0015i$. Control input device and feedback microphone sensor were collocated at 31·5 cm away from the disturbance noise source end. The feedback sensor was a Bruel and Kjaer Type 4187 0·25-in condenser microphone which could detect the sound pressure in the tube and would generate a signal filtered by a home-made filter to a feedback controller. This feedback controller was implemented with a TMS320C25 digital signal processor (DSP) and its interfaces of analogy to digital (A/D) and digital to analogy (D/A) conversions. The control input device was another home-made 8-cm diameter (control) speaker driven by a DENON

PMA-1080R amplifier and produced controlled mass flow rate through a 0·1-m long PVC side tube into the main tube. This set-up is considered to be a collocated structure along the main tube direction. In our experimental set-up the location of microphone is 15 cm away from that of the control speaker, thus, allowing to reduce the influences associated with a real collocated structure like near field effect, directivity and space constraints.

Since we were not able to measure the mass flow rate from the control input device, an identification technique was therefore used to evaluate the associated effects resulting from the actuating system (including the DENON PMA-1080R amplifier, the control input speaker, the side tube, the filter and the A/D component) as shown in Figure 10. The delay due to the DSP and the D/A operations in Figure 9 was not included here. Experiments were carried out from 40 to 700 Hz at every 5 Hz to obtain $\hat{y}_r(\omega, z)/\hat{E}(\omega)$. At the same time, $\hat{y}_r(\omega, z)/\hat{M}(\omega) = \hat{y}_r(i\omega, z)/\hat{M}(i\omega)$ was also calculated by using the theoretical equations (9)–(10) and $K = 0{\cdot}051 - 0{\cdot}0015i$ from 40 to 700 Hz at every 5 Hz. Given the assumption that

$$\frac{\hat{M}(\omega)}{\hat{E}(\omega)} = \frac{\hat{y}_r(\omega, z)}{\hat{E}(\omega)} \cdot \frac{\hat{M}(\omega)}{\hat{y}_r(\omega, z)},$$

then one can obtain $\hat{M}(\omega)/\hat{E}(\omega)$ to estimate the corresponding dynamic and static effects. Two positions, 31·5 and 77·5 cm, were located for a microphone mounting in the experiments. As shown in Figure 11, results of these two corresponding identifications agreed quite well except for frequencies near 190, 400, and 580 Hz. It was unclear why there was such a disagreement at these frequencies. Nevertheless, for those other frequencies, these results demonstrated the static effects of the actuating system for the corresponding disturbance noise. Since the actuating system had a smaller value phase difference (about 18°) at 150 Hz compared with that at other frequencies, we thus focused on the study of active noise control for 150-Hz disturbance noise.

(1) Active noise control without phase compensation

Without consideration of the influence of the actuating system, an LQG controller was designed based on equations (11)–(12) where $N = N_d = 2$. Nominal values of $K = 0{\cdot}051$ and $z_i = z_m = 0{\cdot}315$ m were used in the design. Design parameters were chosen as $q = 10$, $q_{e1} = 1$, and $q_{e2} = 10^3$. A discrete-time transfer function of the designed controller was obtained as

$$G_C(z) =$$

$$\frac{-2{\cdot}8455z^{-1}}{1 \div 0\partial 002446z^{-1}} + \frac{0{\cdot}000708z^{-1}}{1 - 0{\cdot}99706z^{-1}} + \frac{0{\cdot}000297z^{-1}}{1 - 0{\cdot}99874z^{-1}} + \frac{0{\cdot}01304z^{-1} - 0{\cdot}01292z^{-2}}{1 - 1{\cdot}9799z^{-1} + 0{\cdot}9961z^{-2}},$$

by using the 10 K-Hz sampling rate. The discrete-time controller was implemented with a TMS320C25 DSP which could execute an assembly language program of a fixed point arithmetic (Figure 9). We chose 32-bits resolution to represent a real number in our assembly language program since no insertion loss was obtained

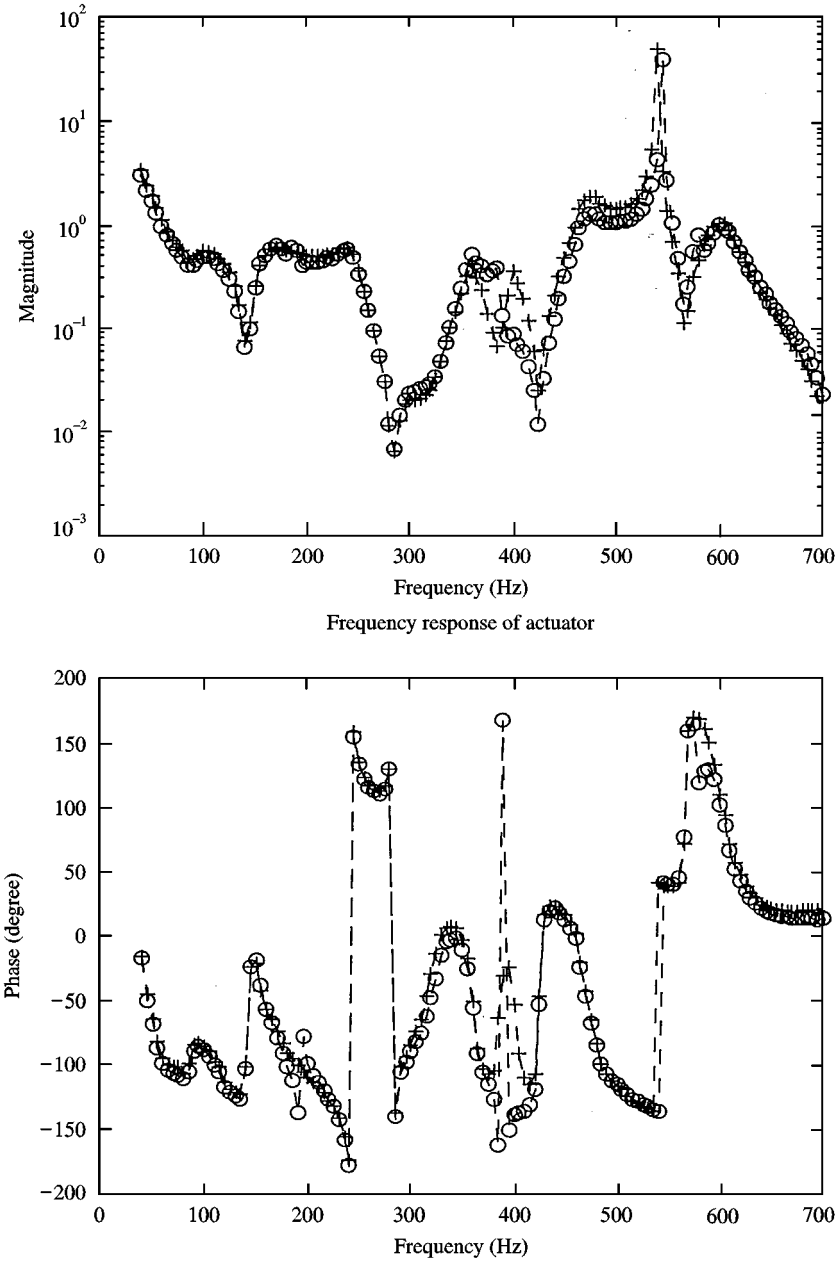

Figure 11. Bode plots of an acutating system: ○, $Zm = 31{\cdot}5$ cm, +, $Zm = 77{\cdot}5$ cm.

upon using 16-bits resolution. The magnitude difference for frequency at 150 Hz in Figure 11 was compensated by manually adjusting the amplifier gain. As shown in Figure 12, the measured steady state response of the sound pressure (voltage) at the feedback-sensor location of the controlled system was compared with that of the uncontrolled system, demonstrating a reducing amplitude for the controlled system. An insertion loss of $-8{\cdot}47$ dB was then obtained according to equation (26).

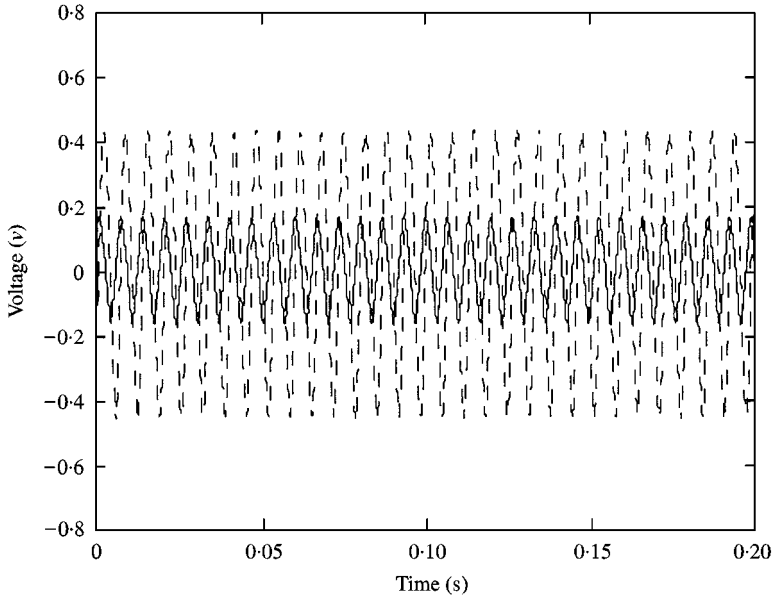

Figure 12. Steady state responses at feedback-sensor location: – – –, Uncontrolled, ——, Controlled.

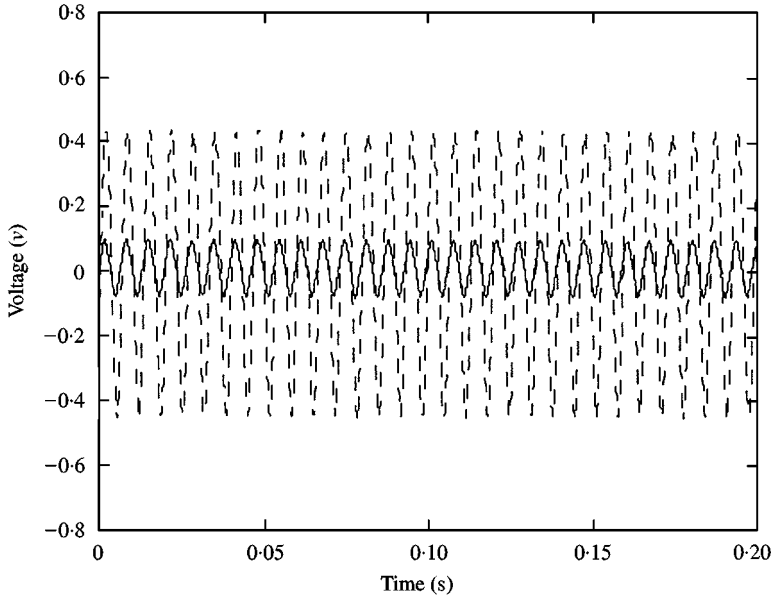

Figure 13. Steady state responses at feedback-sensor location: – – –, Uncontrolled; ——, controlled.

(2) Active noise control with phase compensation

An 18° phase was compensated to the frequency response of the above LQG controller. The compensated frequency response was realized as a compensated controller. A discrete-time transfer function of the compensated controller was

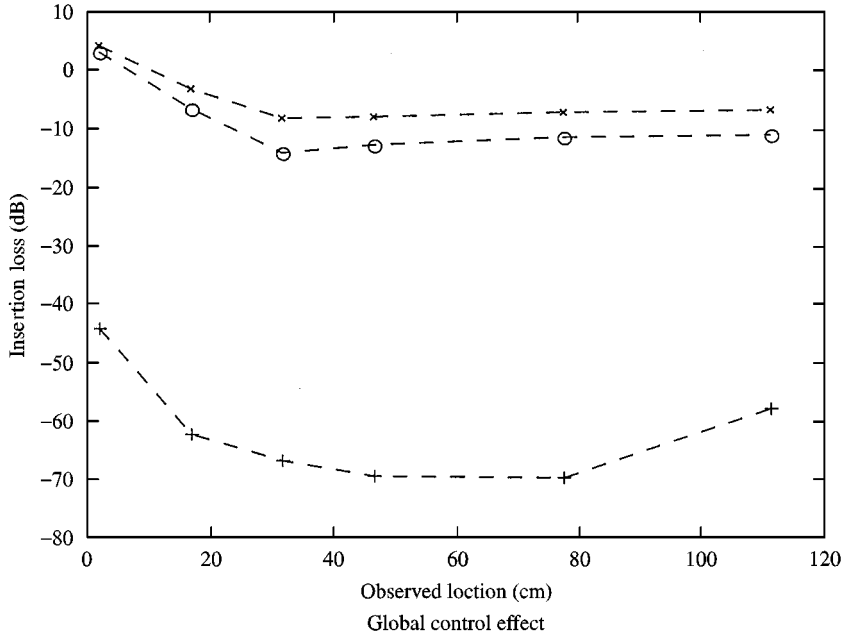

Figure 14. Global noise attenuation: ×: without phase compensation; ○: with phase compensation; +: simulation.

obtained as

$$G_C(z) = \frac{-3{\cdot}6312z^{-1}}{1-0{\cdot}5122z^{-1}} + \frac{-0{\cdot}35052z^{-1}}{1-0{\cdot}7296z^{-1}} + \frac{0{\cdot}4344z^{-1}}{1-0{\cdot}9345z^{-1}} + \frac{0{\cdot}00817z^{-1}-0{\cdot}0093z^{-2}}{1-1{\cdot}9802z^{-1}+0{\cdot}9964z^{-2}}$$

again using 10 K-Hz sampling rate. The steady state response of the controlled system was measured and was shown in Figure 13. A much better insertion loss ($-13{\cdot}8$ dB) was observed as compared with $-8{\cdot}47$ dB in the previous design (Figure 12) without phase compensation.

To examine global control effects of both designs, a second Bruel and Kjaer Type 4187 0·25-in condenser microphone was mounted at different locations (2, 17, 4·5, 77·5 and 111·5 cm) along the main tube to monitor sound pressure. As shown in Figure 14, the modified design with phase compensation ("o" line) had a better insertion loss (additional $-5{\cdot}3$ dB) than that of the design without phase compensation ("x" line) at each of the locations along the main tube, demonstrating a significantly better global performance for this modified design.

By use of the same design parameters in experiments ($q = 10$, $q_{e1} = 1$, and $q_{e2} = 10^3$), the theoretical performance of this design controller was obtained from computer simulation (Figure 14 " + " line). A comparison of insertion loss between the experiment and simulation results indicates a global noise attenuation after the control input point, despite ~ 50 dB differences along the main tube. One major factor for such differences might be the numerical errors produced from the DSP

controller using a fixed point arithmetic. Other factors including delay in the DSP controller, manual adjusting of the amplifier gain, error of the acoustic impedance and unmodelled dynamics of the actuator (speaker) might also contribute to these differences.

7. CONCLUSION

An LQG/GA method is proposed to design active noise controllers. The design parameters in this method are automatically adjusted by using a simple genetic algorithm (SGA) to achieve a better global control performance. A fitness function of LQG/GA specified by a control objective is used to guide the adjustment of those design parameters. A collocated control structure is found to be more useful to obtain stabilizing LQG/GA controllers. The LQG/GA controller has good performance in terms of both disturbance noise rejection and good robustness with respect to the uncertainty of the acoustic impedance. Results of computer simulation show the global control effect in the acoustic duct system after the collocated position of control input and feedback sensor. Results of experiments also support the feasibility of the developed design method. Dynamic effect of an actuating system is not considered in this report and it should be properly modelled and considered in active noise control design in practice.

ACKNOWLEDGMENT

This work was supported by the National Science Council of the Republic of China under the contract of NSC 86-2221-E-005-006.

REFERENCES

1. S.-W. Kang and Y.-H. Kim 1997 *Journal of Sound and Vibration* **201**, 595–611. Active intensity control for the reduction of radiated duct noise.
2. S. D. Sommerfeldt and P. J. Nashif 1994 *Journal of the Acoustical Society of America* **96**, 300–306. An adaptive filtered-x algorithm for energy-based active control.
3. M. L. Manjal and L. J. Eriksson 1998 *Journal of the Acoustic Society of America* **84**, 1086–1093. An analytical, one-dimensional, standing-wave model of a linear active noise control system in a duct.
4. J. Tichy, G. E. Warnaka and L. A. Poole 1984 *Journal of Vibration, Acoustics, Stress, and Reliability in Design* **106**, 399–404. A study of active control of noise in ducts.
5. M. C. J. Trinder and P. A. Nelson 1983 *Journal of Sound and Vibration* **89**, 95–105. Active noise control in finite length ducts.
6. J. S. Hu 1995 ASME *Journal of Dynamic Systems, Measurement, and control* **117**, 143–154. Active sound attenuation in finite-length ducts using close-form transfer function model.
7. A. J. Hull, C. J. Radcliffe and S. C. Southward 1993 ASME *Journal of Dynamic Systems, Measurement, and Control* **115**, 488–494. Global active noise control of a one-dimensional acoustic duct using a feedback controller.
8. A. J. Hull, C. J. Radcliffe, M. Miklavcic and C. R. MacCluer 1990 ASME *Journal of Vibration and Acoustics* **112**, 484–488. State space representation of the nonself-adjoint acoustic duct system.

9. Brian D. O. Anderson and John B. Moore 1990 *Optimal Control*: *Linear Quadratic Methods*. Englewood Cliffs, NJ: Prentice-Hall.
10. Frank L. Lewis and Vassilis L. Syrmos 1995 *Optimal Control*. New York: Wiley.
11. John J. Grefenstette 1986 *IEEE Transaction On Systems, Man, and Cybernetics* SMC-**16**, 122–128. Optimization of control parameters for genetic algorithms.
12. David E. Goldberg 1989 *Genetic Algorithms in Search, Optimization, and Machine Leaning*. New York: Addison-Wesley.
13. K. Kristinsson and G. A. Dumont 1992 *IEEE Transaction On Systems, Man, and Cybernetics* **22**, 1033–1046. System identification and control using genetic algorithms.
14. D. A. Linkens and H. O. Nyongesa 1995 *IEEE Proceeding of Control Theory Application* **142**, 177–185. Genetic algorithms for fuzzy control: Part 2 online system development and application.
15. P. E. Doak 1973 *Journal of Sound and Vibration* **31**, 1–72. Excitation, transmission and radiation of sound from source distributions in hard-walled ducts of finite length (I): the effects of duct cross-section geometry and source distribution space-time pattern.
16. William W. Seto 1971 *Theory and Problem of Acoustics*. New York: McGraw-Hill.
17. Donald E. Baxa 1989 *Noise Control in Internal Combustion Engines*. Malabar, FL: Krieger.

APPENDIX A: DEVELOPMENT OF A REAL STATE-SPACE MODEL

From reference [8], the acoustic duct model of equations (1)–(4) can be transformed to differential equations as

$$\dot{a}_n(t) - c\lambda_n a_n(t) = \left[\frac{-1}{2c\lambda_n L\rho}\right]P(t) + \left[\frac{\psi_n(z_i)}{4c\lambda_n L\rho S}\right]\frac{\partial M(t)}{\partial t}, \quad n = 0, \pm 1, \pm 2, \ldots \tag{A1}$$

$$P(z_m, t) = -\rho c^2 \sum_{n=-\infty}^{\infty} [\lambda_n \psi_n(z_m)]\, a_n(t), \tag{A2}$$

where

$$\lambda_n = \alpha + i(\gamma \to \beta_n), \qquad a_n(t) = \mathrm{e}^{c\lambda_n t}, \qquad \psi_n(z) = \mathrm{e}^{\lambda_n z} - \mathrm{e}^{-\lambda_n z}.$$

Define

$$\bar{x}_0 = \lambda_0 a_0, \qquad \tilde{x}_n = \begin{bmatrix} \lambda_n a_n \\ \lambda_{-n} a_{-n} \end{bmatrix}, \quad n = 1, 2, \ldots.$$

Also, let

$$\bar{A}_0 = c\lambda_0 = \bar{A}_{0r} + i\bar{A}_{0i}, \qquad \bar{B}_0 = \frac{\psi_0(z_i)}{4cL\rho S} = \bar{B}_{0r} + i\bar{B}_{0r},$$

$$\bar{C}_0 = -\rho c^2 \psi_0(z_m) = \bar{C}_{0r} + i\bar{C}_{0i}, \qquad \bar{G}_0 = \frac{-1}{2cL\rho},$$

where

$$\bar{A}_{0r} = c\alpha, \qquad \bar{A}_{0i} = c\gamma,$$

$$\bar{B}_{0r} = \frac{\cos\gamma z_i \sinh\alpha z_i}{2cL\rho S}, \qquad \bar{B}_{0i} = \frac{\sin\gamma z_i \cosh\alpha z_i}{2cL\rho S},$$

$$\bar{C}_{0r} = -2\rho c^2 \cos\gamma z_m \sinh\alpha z_m, \qquad \bar{C}_{0i} = -2\rho c^2 \sin\gamma z_m \cosh\alpha z_m.$$

Then equations (A1)–(A2) can be rewritten as

$$\dot{\bar{x}}_0(t) = \bar{A}_0 \bar{x}_0(t) + \bar{B}_0 u(t) + \bar{G}_0 d(t), \tag{A3}$$

$$\dot{\tilde{x}}_n(t) = \tilde{A}_n \tilde{x}_n(t) + \tilde{B}_n u(t) + \tilde{G}_n d(t), \quad n = 1, 2, \ldots, \tag{A4}$$

$$y(t) = \bar{C}_0 \bar{x}_0(t) + \sum_{n=1}^{\infty} \tilde{C}_n \tilde{x}_n(t), \tag{A5}$$

where for $n = 1, 2, \ldots,$

$$\tilde{A}_n = \begin{bmatrix} c\lambda_n & 0 \\ 0 & c\lambda_{-n} \end{bmatrix}, \qquad \tilde{B}_n = \frac{1}{4cL\rho S} \begin{bmatrix} \psi_n(z_i) \\ \psi_{-n}(z_i) \end{bmatrix},$$

$$\tilde{C}_n = -\rho c^2 [\psi_n(z_m) \quad \psi_{-n}(z_m)], \qquad \tilde{G}_n = \frac{-1}{2cL\rho} \begin{bmatrix} 1 \\ 1 \end{bmatrix}.$$

Define

$$p = \begin{bmatrix} 1 & 1 \\ i & -i \end{bmatrix}$$

For $n = 1, 2, \ldots,$ let

$$\bar{A}_n = p\tilde{A}_n p^{-1} = \bar{A}_{nr} + i\bar{A}_{ni}, \qquad \bar{B}_n = p\tilde{B}_n = \bar{B}_{nr} + i\bar{B}_{ni},$$

$$\bar{C}_n = \tilde{C}_n p^{-1} = \bar{C}_{nr} + iC_{ni}, \qquad \bar{G}_n = p\tilde{G}_n = \frac{-1}{cL\rho} \begin{bmatrix} 1 \\ 0 \end{bmatrix},$$

where

$$\bar{A}_{nr} = c \begin{bmatrix} \alpha & \beta_n \\ -\beta_n & \alpha \end{bmatrix}, \qquad \bar{A}_{ni} = c\gamma \begin{bmatrix} 1 & 0 \\ 0 & 1 \end{bmatrix},$$

$$\bar{B}_{nr} = \frac{\cos \gamma z_i}{cL\rho S} \begin{bmatrix} \cos \beta_n z_i \sinh \alpha z_i \\ -\sin \beta_n z_i \cosh \alpha z_i \end{bmatrix}, \qquad \bar{B}_{ni} = \frac{\sin \gamma z_i}{cL\rho S} \begin{bmatrix} \cos \beta_n z_i \cosh \alpha z_i \\ -\sin \beta_n z_i \sinh \alpha z_i \end{bmatrix},$$

$$\bar{C}_{nr} = -2\rho c^2 \cos \gamma z_m [\cos \beta_n z_m \sinh \alpha z_m \sin \beta_n z_m \ \cosh \alpha z_m],$$

$$\bar{C}_{ni} = -2\rho c^2 \sin \gamma z_m [\cos \beta_n z_m \cosh \alpha z_m \sin \beta_n z_m \ \sinh \alpha z_m].$$

Define $\bar{x}_n = p\tilde{x}_n$ for $n = 1, 2, \ldots$. Then the system of equations (A3)–(A5) can be represented as

$$\dot{\bar{x}}_n = \bar{A}_n \bar{x}_n + \bar{B}_n u + \bar{G}_n d, \qquad n = 0, 1, 2, \ldots, \tag{A6}$$

$$y = \sum_{n=0}^{\infty} \bar{C}_n \bar{x}_n. \tag{A7}$$

Finally, define a state variable in the real space as

$$x_n = \begin{bmatrix} \bar{x}_{nr} \\ \bar{x}_{ni} \end{bmatrix}, \qquad n = 0, 1, 2, \ldots,$$

where $\bar{x}_{nr}$ and $\bar{x}_{ni}$ are the real part and the imaginary part of $\bar{x}_n = \bar{x}_{nr} + i\bar{x}_{ni}$ respectively. Then a real state-space acoustic duct model can be obtained from equations (A6)–(A7) as equations (7)–(8).